Intraband versus interband decoherence times in biased semiconductor superlattices

Aizhen Zhang and M. M. Dignam
Department of Physics, Queen's University, Kingston, Ontario, Canada K7L 3N6
(Received 16 September 2003; published 15 March 2004)

We develop a theoretical method of calculating the dynamics of excitons in biased semiconductor superlattices, including exciton-LO-phonon interactions. We use this method to determine phonon-induced excitonic decoherence in the interband and intraband polarizations. We find that the intraband decoherence time is much longer than one would expect from a simple extrapolation from the interband decoherence time. The longer decoherence time is shown to be due to the persistence of intraband coherence after exciton-phonon scattering events. The results are found to be in qualitative agreement with recent experiments.

DOI: 10.1103/PhysRevB.69.125314 PACS number(s): 78.47.+p, 73.21.−b, 78.67.−n

I. INTRODUCTION

There has been considerable interest in recent years in the excitation of semiconductors via ultrashort optical pulses.[1–13] The optical excitation of a semiconductor creates both an interband polarization and an intraband polarization. Scattering processes tend to destroy the coherence, leading to a temporal decay of both polarizations. Typical time scales for decoherence in semiconductors are in the range of a few hundred femtoseconds to a few picoseconds. With the enormous progress in ultrashort experimental techniques in recent years, a wide variety of phenomena related to relaxation and transport dynamics has been investigated, both experimentally and theoretically, in bulk semiconductors as well as in lower-dimensional semiconductors. The most commonly used experimental techniques for these studies have been four-wave-mixing (FWM) experiments and the detection of coherently emitted terahertz (THz) radiation (THz emission spectroscopy). These methods respectively provide direct information on interband and intraband polarization dynamics.

One dynamic process that has been the subject of extensive experimental and theoretical work in recent years is Bloch oscillations (BO's). In 1928, Bloch[14] demonstrated that in the absence of interband tunneling and scattering processes, an electron in a periodic potential subject to an external static electric field F_0 oscillates at a frequency $\omega_B = edF_0/\hbar$, undergoing the so-called Bloch oscillations. Correspondingly, the energy spectrum was shown to consist of the so-called Wannier-Stark[15] ladder (WSL) with energies $E_n = E_0 + nedF_0$. For many years the very existence of BO's and the WSL was a point of controversy. A dramatic advance in the potential to observe BO's and the WSL came with the invention of the semiconductor superlattice (SL). The main advantage of the SL is the large lattice constant, which leads to (mini)bandwidths much smaller than those of the underlying crystal lattice. This results in a smaller BO period for a given electric field. Thus for modest electric fields, the carriers can execute a number of BO's before the coherence is destroyed by scattering. To date, the existence of the WSL (Refs. 16 and 17) as well as BO's (Refs. 18–23) in superlattices has been confirmed by a number of experiments. BO's have been detected by monitoring the interband polarization,[19,20] intraband polarization,[21] and terahertz radiation.[22,23]

The experimental investigations into the interband and intraband dynamics in biased semiconductor superlattices (BSSL's) have been accompanied by considerable theoretical activity.[24–34] One of the first theoretical treatments of intraband dynamics in a BSSL employed the semiconductor Bloch equations (SBE's) in the Hartree-Fock (HF) approximation[24] with phenomenological interband (T_{inter}) and intraband (T_{intra}) decoherence times. A later calculation by Axt *et al.*, which employed dynamics controlled truncation theory (DCT),[26] showed that the use of the HF approximation in the SBE's leads to incorrect intraband dynamics except in the so-called coherent limit, where $T_{inter} = 2T_{intra}$. This was later verified experimentally by Bolivar *et al.*,[35] where they also observed that the BSSL that they were studying was far from the coherent limit, with $T_{inter} \simeq \frac{2}{3} T_{intra}$.

Later calculations[25,28] also employed the SBE's but with the inclusion of carrier-phonon scattering in the Markov approximation. The inclusion of an explicit decoherence mechanism alleviates some of the problems associated with the HF approximation. In fact, if one assumes that decoherence is only due to carrier-phonon scattering, then if this interaction is treated exactly, the results using the SBE's (or DCT theory) will be exact for any choice of basis states. Only when approximations are made in the treatment of the interaction will the choice of method or basis affect the results. Unfortunately, the coupled carrier-phonon system is sufficiently complex so that one must always make considerable approximations (such as the Markov approximation) to make it computationally tractable. Therefore the choice of basis and method (SBE or DCT, for example) will have an effect on the results. This issue was treated convincingly by Hader *et al.*,[28] who calculated the BSSL dynamics in the presence of electron-phonon scattering in the Markov approximation using the SBE's with two different bases: the usual single-particle Bloch-state basis and the single-particle Wannier-Stark basis. The authors found that even at moderate static field strengths ($\sim$15 kV/cm), the results for intraband decoherence times depended rather strongly on the basis used. This is because the Markov approximation[36] effectively involves the assumption that the particles remain in one of the states in the chosen basis during the scattering process. It is thus clear that the closer the basis states are to the true eigenstates of the particles, the more accurate the

 ©2004 The American Physical Society

results will be. Thus, as pointed out by Hader *et al.*,[28] for the BSSL, the Wannier-Stark basis will yield more accurate results than the Bloch-state basis when a static field is present. Extrapolating this result, one is led to the conclusion that the use of a basis consisting of the *excitonic* states of the BSSL should yield more accurate results still. This is the approach that we take here, where we employ DCT theory with an excitonic basis to calculate the intraband response to second order in the optical field in the presence of carrier-LO-phonon scattering.

An excitonic basis has been employed by a number of authors in treating coherent dynamics in BSSL's. Lachaine *et al.*[29] employed the excitonic basis to investigate the intraband polarization of a SL in combined dc and ac fields. The excitonic basis has also been employed recently to study FWM (Ref. 30) and dynamic localization[31] in a BSSL. In all of these works, exciton-phonon interactions were neglected and phenomenological decoherence times for the interband and intraband polarizations were employed. Zhang *et al.*[37] calculated the effects of acoustic phonons and disorder on the THz emission from small number of coupled semiconductor quantum wells using the exciton representation. However, so far no detailed theoretical study of the dynamics of phonon-induced interband and intraband decoherence in an optically excited BSSL has been given.

One major motivation of this work is to obtain a better understanding of the origins of interband and intraband decoherence. As mentioned above, Bolivar *et al.*[35] recently found experimentally that for the BSSL studied, $T_{inter} \simeq \frac{2}{3} T_{intra}$. This would appear to be in contradiction to a simple picture wherein (as we shall later show) one would expect the decoherence times to obey the coherent expression, $T_{inter} = 2T_{intra}$. In order to understand the source of this strong deviation from the coherent limit, we consider the exciton dynamics in the presence of decoherence.

The destruction of coherence can be caused by various scattering mechanisms such as carrier-carrier scattering, disorder scattering, and carrier-phonon scattering. When the bandwidth is larger than the phonon energy, the dominant mechanisms at low temperatures and low carrier density are scattering from disorder and from longitudinal optical (LO) phonons. In this paper we will neglect the effects of disorder and consider the decoherence arising from the interaction of excitons with LO phonons. We derive a closed set of equations of motion describing the interband and intraband correlation functions to second order in the optical field, using the Markov approximation. Employing this model, we study the decoherence mechanisms for the interband and intraband polarizations, with particular emphasis on intraband dynamics. We find that while interband coherence is essentially completely destroyed when an exciton is scattered via a phonon, the intraband coherence is only reduced by a relatively small amount. This difference arises from the different dependence of the two polarizations on the center-of-mass wave vector $\mathbf{K}$. When the excitons are scattered from a $\mathbf{K}=\mathbf{0}$ state to a $\mathbf{K}\neq\mathbf{0}$ state via phonons, the interband polarization is completely destroyed. In contrast, the intraband coherence is only modestly affected, since the scattered $\mathbf{K}\neq\mathbf{0}$ excitons can continue to oscillate and emit THz radiation. The net result is that rather than finding $T_{intra}=T_{inter}/2$, we find $T_{intra}\simeq T_{inter}$ in qualitative agreement with experiment.[35]

The paper is organized as follows. In Sec. II we introduce the model and the equations of motion of the coupled exciton-phonon system, and give an outline of the numerical implementation. In Sec. III, we present the numerical results for the interband polarization, the intraband polarization, and the THz signal. A summary is given in Sec. IV.

II. THE MODEL AND THEORETICAL APPROACH

We investigate the dynamics of a semiconductor superlattice in an applied dc electric field, photoexcited by an ultrashort ($\sim$100 fs) optical pulse. We employ the quasi-bosonic formalism of Hawton and Nelson[38] that has previously been successfully applied to the calculation of interband and intraband dynamics of BSSL's.[29–32,34] Using an excitonic basis, a set of dynamic equations for interband and intraband correlation functions to second order in the optical field is derived including exciton-LO-phonon interactions. We begin with a presentation of the Hamiltonian, followed by a derivation of the dynamical equations and the numerical implementation.

A. The Hamiltonian

Working in an excitonic basis,[30] the physical system can be described by the following Hamiltonian:

$$H(t) = H_0 + H_{op} + H_{ph} + H_{int}. \tag{1}$$

In this expression,

$$H_0 = \sum_{\mu,\mathbf{K}} E_\mu^{\mathbf{K}} B_{\mu,\mathbf{K}}^+ B_{\mu,\mathbf{K}} \tag{2}$$

is the Hamiltonian for noninteracting superlattice excitons *in the presence of a dc electric field* F_0, where $B_{\mu,\mathbf{K}}^+$ ($B_{\mu,\mathbf{K}}$) is the creation (annihilation) operator for an exciton with center-of-mass (c.m.) wave vector $\mathbf{K}$, internal quantum number μ, and energy $E_\mu^{\mathbf{K}}$. To simplify the calculations, we assume a parabolic dispersion for the c.m. dependence of the exciton energy:

$$E_\mu^{\mathbf{K}} \simeq E_\mu^{\mathbf{0}} + \frac{\hbar^2 K_z^2}{2M_z} + \frac{\hbar^2 K_\parallel^2}{2M_\parallel}, \tag{3}$$

where M_z is the c.m. excitonic effective mass in the z direction and $M_\parallel$ is the c.m. excitonic effective mass parallel to the layers. The term

$$H_{op} = -V\mathbf{E}_{op}(t)\cdot\mathbf{P}_{inter} \tag{4}$$

is the interaction Hamiltonian between the optical field $\mathbf{E}_{op}(t)$ and the excitons, where V is the volume of the system and $\mathbf{P}_{inter}$ is the interband polarization operator defined by

$$\mathbf{P}_{inter} = \frac{1}{V}\sum_\mu [\mathbf{M}_\mu B_{\mu,0}^+ + \mathbf{M}_\mu^* B_{\mu,0}]. \tag{5}$$

Here,

$$\mathbf{M}_{\mu}=\mathbf{M}_{o}A\int dz\Phi^{*}_{\mu,\mathbf{0}}(z,z,0) \tag{6}$$

is the interband dipole matrix element, where $\mathbf{M}_o$ is the bulk interband dipole matrix element, A is the transverse area, and $\Phi_{\mu,\mathbf{K}}$ is the envelope function of the SL exciton eigenstate in the presence of the dc electric field with quantum numbers $(\mu,\mathbf{K})$. We consider excitation via ultrashort Gaussian optical pulses with central frequency ω_c and duration τ_p. Hence the optical field is given by

$$\mathbf{E}_{opt}=\mathbf{A}_0 e^{-(t/\tau_p)^2}e^{-i\omega_c t}+\text{c.c.}. \tag{7}$$

In writing the full Hamiltonian, we have assumed that the exciton density is low enough that we can neglect exciton-exciton interactions, and in what follows we will similarly neglect phase spacing filling and treat the excitons as bosons. Both assumptions are rigorously valid to second order in the optical field.[30]

The term

$$H_{ph}=\sum_{\mathbf{q}}\hbar\omega_{\mathbf{q}}b^{+}_{\mathbf{q}}b_{\mathbf{q}} \tag{8}$$

describes the free-phonon dynamics, where $\hbar\omega_{\mathbf{q}}$ is the energy of the LO phonon with wave vector $\mathbf{q}$, and $b^{+}_{\mathbf{q}}$ and $b_{\mathbf{q}}$ denote the creation and annihilation operators for this phonon. For simplicity, we consider a single dispersionless bulk LO-phonon mode only so that $\omega_{\mathbf{q}}=\omega_{LO}$. Previous investigations have shown that the scattering rates are sufficiently well reproduced if the phonon spectrum is assumed to be bulklike.[39]

The coupling between carriers and phonons is described by the Hamiltonian

$$H_{cp}=\int d\mathbf{r}\boldsymbol{\Psi}^{+}(\mathbf{r})V_{cp}(\mathbf{r})\boldsymbol{\Psi}(\mathbf{r}), \tag{9}$$

where $\boldsymbol{\Psi}^{+}(\mathbf{r})$ and $\boldsymbol{\Psi}(\mathbf{r})$ are the field operators and

$$V_{cp}(\mathbf{r})=\sum_{\mathbf{q}}\left[g_{\mathbf{q}}b_{\mathbf{q}}e^{i\mathbf{q}\cdot\mathbf{r}}+g^{*}_{\mathbf{q}}b^{+}_{\mathbf{q}}e^{-i\mathbf{q}\cdot\mathbf{r}}\right] \tag{10}$$

is the potential induced by the lattice. The explicit form of the coupling function $g_{\mathbf{q}}$ depends on the particular phonon branch (acoustic, optical, etc.) as well as on the coupling mechanism considered (deformation potential, polar coupling, etc.). We discuss only the interaction with optical phonons via Fröhlich interaction, which is the most important type of carrier-phonon interaction for ultrafast dynamics for the structure and dc field considered here. In this case,

$$g^{2}_{\mathbf{q}}=\frac{\hbar\omega_{LO}}{2V}\frac{e^2}{\epsilon_0 q^2}\left(\frac{1}{\epsilon_\infty}-\frac{1}{\epsilon_s}\right), \tag{11}$$

where $q=|\mathbf{q}|$, ϵ_∞ and ϵ_s are the high-frequency and static limits of the relative dielectric constant, respectively, and ϵ_0 is the vacuum dielectric constant. We expand the second-quantization field operators in terms of the wave functions for conduction- and valence-band electrons as

$$\boldsymbol{\Psi}(\mathbf{r})=\sum_{\lambda=(c,v),\mathbf{k}}a_{\lambda,\mathbf{k}}\psi_{\lambda,\mathbf{k}}(\mathbf{r}), \tag{12}$$

where $a_{\lambda,\mathbf{k}}$ is the annihilation operator for an electron in the state $\psi_{\lambda,\mathbf{k}}(\mathbf{r})$ in band λ with wave vector $\mathbf{k}$. After the transformation from electron and hole operators to exciton operators,[38] the exciton-phonon interaction finally adopts the form

$$H_{int}=\sum_{\mathbf{K},\mathbf{q},\mu,\mu'}Q(\mu,\mu',\mathbf{K},\mathbf{q})B^{+}_{\mu,\mathbf{K}+\mathbf{q}}B_{\mu',\mathbf{K}}b_{\mathbf{q}}+Q^{*}(\mu,\mu',\mathbf{K},\mathbf{q})B^{+}_{\mu,\mathbf{K}-\mathbf{q}}B_{\mu',\mathbf{K}}b^{+}_{\mathbf{q}} \tag{13}$$

with

$$Q(\mu,\mu',\mathbf{K},\mathbf{q})=g_{\mathbf{q}}\sum_{\mathbf{k}}\left[(\varphi^{\mu,\mathbf{K}+\mathbf{q}}_{\mathbf{k}+\alpha_h\mathbf{q}})^{*}\varphi^{\mu',\mathbf{K}}_{\mathbf{k}}-(\varphi^{\mu,\mathbf{K}+\mathbf{q}}_{\mathbf{k}})^{*}\varphi^{\mu',\mathbf{K}}_{\mathbf{k}+\alpha_e\mathbf{q}}\right], \tag{14}$$

where $\mathbf{K}$ is the c.m. wave vector of the exciton, $\mathbf{k}$ is the relative electron-hole wave vector, $\varphi^{\mu,\mathbf{K}}_{\mathbf{k}}$ are the expansion coefficients of the exciton envelope functions $\Phi_{\mu,\mathbf{K}}$ in the free electron-hole basis, and $\alpha_e\equiv m_e/M=m_e/(m_e+m_h)$ and $\alpha_h\equiv m_h/M$ denote the relative electron and hole masses, respectively. The first and second terms in Eq. (13) simply correspond, respectively, to phonon absorption and emission by excitons.

In order to proceed with the calculations, we must determine the superlattice excitonic states in the presence of the dc electric field. This is accomplished by using the two-well excitonic method of Dignam and Sipe.[40] To determine which excitonic states to include in basis, we note first that although only excitons with zero center-of-mass momentum will be optically excited, phonons will scatter those excitons into states with $\mathbf{K}\neq\mathbf{0}$. Thus we must include $\mathbf{K}\neq\mathbf{0}$ states in our basis. Second, if the exciting laser pulse has an energy spectrum centered below the energy of the $n=0$ $1s$ excitonic WSL state, it has been shown[33,34] that predominantly $1s$-like excitons are optically created and that the excitonic states with excited in-plane motion can be neglected. Thus in this paper we will only consider the scattering taking place between $1s$ excitons with different $\mathbf{K}$ and along-axis internal quantum numbers. Although phonons can scatter optically created excitons into states with higher in-plane quantum numbers $(2s,3s,\ldots)$, we find that the matrix elements and energy conservation are such that these events are expected to contribute little over the first few picoseconds. Thus we neglect these states with higher in-plane motion.

B. Equations of motion

We wish to now calculate the interband and intraband dynamics of the system excited by the optical pulse. The interband polarization is given by the expectation value of Eq. (5) while the spatially uniform part of the intraband polarization is given by

$$\mathbf{P}_{intra}=\frac{1}{V}\sum_{\mu,\nu,\mathbf{K}}\mathbf{G}_{\mu\nu}\langle B^{+}_{\mu,\mathbf{K}}B_{\nu,\mathbf{K}}\rangle, \tag{15}$$

where $\mathbf{G}_{\mu\nu}$ is the intraband dipole matrix element between two excitonic states $|\Phi_{\mu,\mathbf{K}}\rangle$ and $|\Phi_{\nu,\mathbf{K}}\rangle$, and is given approximately by[30]

$$\mathbf{G}_{\mu\nu}=\langle\Phi_{\mu,\mathbf{0}}|-e(\mathbf{r}_e-\mathbf{r}_h)|\Phi_{\nu,\mathbf{0}}\rangle. \tag{16}$$

Note that due to the requirement of momentum conservation, the interband polarization only depends on $\langle B_{\mu,0}\rangle$ and not on $\langle B_{\mu,\mathbf{K}}\rangle$ for $\mathbf{K}\neq\mathbf{0}$. On the other hand, the intraband polarization depends on contributions from $\langle B^{+}_{\mu,\mathbf{K}}B_{\nu,\mathbf{K}}\rangle$ for all $\mathbf{K}$. This crucial difference is the main source of difference between the interband and intraband decoherence, as we shall show.

The equations of motion for the expectation values of these interband and intraband correlation functions to second order in the optical field are[30]

$$i\hbar\frac{d\langle B_{\mu,0}\rangle}{dt}=E^{0}_{\mu}\langle B_{\mu,0}\rangle-\mathbf{E}_{opt}\cdot\mathbf{M}_{\mu}+i\hbar\frac{d\langle B_{\mu,0}\rangle}{dt}|_{scatt} \tag{17}$$

$$i\hbar\frac{d\langle B^{+}_{\mu,\mathbf{K}}B_{\nu,\mathbf{K}}\rangle}{dt}=(E^{\mathbf{K}}_{\nu}-E^{\mathbf{K}}_{\mu})\langle B^{+}_{\mu,\mathbf{K}}B_{\nu,\mathbf{K}}\rangle+\mathbf{E}_{opt}\cdot[\mathbf{M}^{*}_{\mu}\langle B_{\nu,0}\rangle-\mathbf{M}_{\nu}\langle B^{+}_{\mu,0}\rangle]+i\hbar\frac{d\langle B^{+}_{\mu,\mathbf{K}}B_{\nu,\mathbf{K}}\rangle}{dt}|_{scatt}, \tag{18}$$

where the exciton-phonon scattering terms yield the following contributions to the equations of motion:

$$i\hbar\frac{d\langle B_{\mu,0}\rangle}{dt}|_{scatt}=\sum_{\mathbf{q},\mu'}Q(\mu,\mu',-\mathbf{q},\mathbf{q})\langle B_{\mu',-\mathbf{q}}b_{\mathbf{q}}\rangle+Q^{*}(\mu,\mu',\mathbf{q},\mathbf{q})\langle B_{\mu',\mathbf{q}}b^{+}_{\mathbf{q}}\rangle, \tag{19}$$

$$\begin{aligned}i\hbar\frac{d\langle B^{+}_{\mu,\mathbf{K}}B_{\nu,\mathbf{K}}\rangle}{dt}|_{scatt}=&\sum_{\mathbf{q},\mu'}Q(\nu,\mu',\mathbf{K}-\mathbf{q},\mathbf{q})\\&\times\langle B^{+}_{\mu,\mathbf{K}}B_{\mu',\mathbf{K}-\mathbf{q}}b_{\mathbf{q}}\rangle-Q(\mu,\mu',\mathbf{K},\mathbf{q})\\&\times\langle B^{+}_{\mu',\mathbf{K}+\mathbf{q}}B_{\nu,\mathbf{K}}b_{\mathbf{q}}\rangle+Q^{*}(\nu,\mu',\mathbf{K}\\&+\mathbf{q},\mathbf{q})\langle B^{+}_{\mu,\mathbf{K}}B_{\mu',\mathbf{K}+\mathbf{q}}b^{+}_{\mathbf{q}}\rangle\\&-Q^{*}(\mu,\mu',\mathbf{K},\mathbf{q})\langle B^{+}_{\mu',\mathbf{K}-\mathbf{q}}B_{\nu,\mathbf{K}}b^{+}_{\mathbf{q}}\rangle.\end{aligned} \tag{20}$$

Here, new variables, the so-called phonon-assisted operators, have been introduced. These variables describe correlations between excitons and phonons. The equations of motion for the phonon-assisted operators involve expectation values of four operators, and therefore an infinite hierarchy of equations arises. Neglecting the terms which describe phonon-assisted optical transitions and neglecting phonon coherence ($\langle b^{+}_{\mathbf{q}}b_{\mathbf{q}'}\rangle=\langle b^{+}_{\mathbf{q}}b_{\mathbf{q}}\rangle\delta_{\mathbf{q},\mathbf{q}'},\langle b^{+}_{\mathbf{q}}b^{+}_{\mathbf{q}'}\rangle=0$), the equations of motion for the phonon-assisted operators on the right-hand side of Eqs. (19) and (20) to second order are

$$i\hbar\frac{d\langle B_{\mu',-\mathbf{q}}b_{\mathbf{q}}\rangle}{dt}=(E^{-\mathbf{q}}_{\mu'}+\hbar\omega_{\mathbf{q}})\langle B_{\mu',-\mathbf{q}}b_{\mathbf{q}}\rangle+\sum_{\mu''}(n_{\mathbf{q}}+1)Q^{*}(\mu',\mu'',0,\mathbf{q})\langle B_{\mu'',0}\rangle, \tag{21}$$

$$\begin{aligned}i\hbar\frac{d\langle B^{+}_{\mu,\mathbf{K}}B_{\mu',\mathbf{K}-\mathbf{q}}b_{\mathbf{q}}\rangle}{dt}&=(E^{\mathbf{K}-\mathbf{q}}_{\mu'}-E^{\mathbf{K}}_{\mu}+\hbar\omega_{\mathbf{q}})\langle B^{+}_{\mu,\mathbf{K}}B_{\mu',\mathbf{K}-\mathbf{q}}b_{\mathbf{q}}\rangle\\&+\sum_{\mu''}(n_{\mathbf{q}}+1)Q^{*}(\mu',\mu'',\mathbf{K},\mathbf{q})\langle B^{+}_{\mu,\mathbf{K}}B_{\mu'',\mathbf{K}}\rangle,\end{aligned} \tag{22}$$

where we have introduced the factorizations $\langle B_{\mu'',0}b_{\mathbf{q}}b^{+}_{\mathbf{q}}\rangle=\langle B_{\mu'',0}\rangle(n_{\mathbf{q}}+1)$ and $\langle B^{+}_{\mu,\mathbf{K}}B_{\mu'',\mathbf{K}}b_{\mathbf{q}}b^{+}_{\mathbf{q}}\rangle=\langle B^{+}_{\mu,\mathbf{K}}B_{\mu'',\mathbf{K}}\rangle(n_{\mathbf{q}}+1)$. As we finally assume $n_{\mathbf{q}}=0$, this factorization is exact. By applying the Markov approximation,[36] we solve these equations to obtain

$$\langle B_{\mu',-\mathbf{q}}b_{\mathbf{q}}\rangle=-i\pi\sum_{\mu''}\delta(E^{0}_{\mu''}-E^{-\mathbf{q}}_{\mu'}-\hbar\omega_{\mathbf{q}})(n_{\mathbf{q}}+1)Q^{*}(\mu',\mu'',0,\mathbf{q})\langle B_{\mu'',0}\rangle, \tag{23}$$

$$\langle B^{+}_{\mu,\mathbf{K}}B_{\mu',\mathbf{K}-\mathbf{q}}b_{\mathbf{q}}\rangle=-i\pi\sum_{\mu''}\delta(E^{\mathbf{K}}_{\mu''}-E^{\mathbf{K}-\mathbf{q}}_{\mu'}-\hbar\omega_{\mathbf{q}})(n_{\mathbf{q}}+1)Q^{*}(\mu',\mu'',\mathbf{K},\mathbf{q})\langle B^{+}_{\mu,\mathbf{K}}B_{\mu'',\mathbf{K}}\rangle, \tag{24}$$

and similar expressions for other phonon-assisted operators. Here $n_{\mathbf{q}}=\langle b^{+}_{\mathbf{q}}b_{\mathbf{q}}\rangle$ denotes the phonon occupation number. When performing the Markov approximation, the phonon-assisted operators are factorized into a slowly varying part and a rapid-oscillating part. This approximation implies that the carriers stay in their state for the duration of a scattering event. Thus this factorization is only good if the basis states are approximately eigenstates of the carrier Hamiltonian. As we use an excitonic basis we expect this to be a good approximation. To make the calculation as simple as possible, in what follows we assume the temperature and carrier densities are low, and so we take $n_{\mathbf{q}}=0$ (phonon absorption is negligible).

By inserting the explicit form of the various contributions into Eqs. (19) and (20) we can finally write down

$$i\hbar\frac{d\langle B_{\mu,0}\rangle}{dt}|_{scatt}=-i\pi\sum_{\mathbf{q},\mu',\mu''}\delta(E^{0}_{\mu''}-E^{-\mathbf{q}}_{\mu'}-\hbar\omega_{\mathbf{q}})Q(\mu,\mu',-\mathbf{q},\mathbf{q})Q^{*}(\mu',\mu'',0,\mathbf{q})\langle B_{\mu'',0}\rangle \tag{25}$$

and

$$i\hbar\frac{d\langle B^{+}_{\mu,\mathbf{K}}B_{\nu,\mathbf{K}}\rangle}{dt}\Big|_{scatt}=-i\pi\Bigg\{\sum_{\mathbf{q},\mu',\mu''}\delta(E^{\mathbf{K}}_{\mu''}-E^{\mathbf{K}-\mathbf{q}}_{\mu'}-\hbar\omega_{\mathbf{q}})Q(\nu,\mu',\mathbf{K}-\mathbf{q},\mathbf{q})Q^{*}(\mu',\mu'',\mathbf{K},\mathbf{q})\langle B^{+}_{\mu,\mathbf{K}}B_{\mu'',\mathbf{K}}\rangle$$
$$+\sum_{\mathbf{q},\mu',\mu''}\delta(E^{\mathbf{K}}_{\mu''}-E^{\mathbf{K}-\mathbf{q}}_{\mu'}-\hbar\omega_{\mathbf{q}})Q(\mu',\mu'',\mathbf{K}-\mathbf{q},\mathbf{q})Q^{*}(\mu,\mu',\mathbf{K},\mathbf{q})\langle B^{+}_{\mu'',\mathbf{K}}B_{\nu,\mathbf{K}}\rangle\Bigg\}$$
$$+i\pi\Bigg\{\sum_{\mathbf{q},\mu',\mu''}\delta(E^{\mathbf{K}+\mathbf{q}}_{\mu''}-E^{\mathbf{K}}_{\nu}-\hbar\omega_{\mathbf{q}})Q(\mu,\mu',\mathbf{K},\mathbf{q})Q^{*}(\nu,\mu'',\mathbf{K}+\mathbf{q},\mathbf{q})\langle B^{+}_{\mu',\mathbf{K}+\mathbf{q}}B_{\mu'',\mathbf{K}+\mathbf{q}}\rangle$$
$$+\sum_{\mathbf{q},\mu',\mu''}\delta(E^{\mathbf{K}+\mathbf{q}}_{\mu''}-E^{\mathbf{K}}_{\mu}-\hbar\omega_{\mathbf{q}})Q(\mu,\mu'',\mathbf{K},\mathbf{q})Q^{*}(\nu,\mu',\mathbf{K}+\mathbf{q},\mathbf{q})\langle B^{+}_{\mu'',\mathbf{K}+\mathbf{q}}B_{\mu',\mathbf{K}+\mathbf{q}}\rangle\Bigg\}. \quad (26)$$

The only terms in Eq. (25) and in the first and second sums in Eq. (26) that will contribute significantly are the resonant terms. Therefore, we only include the terms where $\mu''=\mu$ in Eq. (25), $\mu''=\nu$ in the first sum, and $\mu''=\mu$ in the second sum in Eq. (26). Thus Eqs. (25) and (26) can be simplified to

$$i\hbar\frac{d\langle B_{\mu,0}\rangle}{dt}\Big|_{scatt}=-i\Gamma_{inter}\langle B_{\mu,0}\rangle \quad (27)$$

and

$$i\hbar\frac{d\langle B^{+}_{\mu,\mathbf{K}}B_{\nu,\mathbf{K}}\rangle}{dt}\Big|_{scatt}=-i\Gamma_{intra}(\mathbf{K})\langle B^{+}_{\mu,\mathbf{K}}B_{\nu,\mathbf{K}}\rangle$$
$$+i\pi\Bigg\{\sum_{\mathbf{q},\mu',\mu''}\delta(E^{\mathbf{K}+\mathbf{q}}_{\mu''}-E^{\mathbf{K}}_{\nu}-\hbar\omega_{\mathbf{q}})Q(\mu,\mu',\mathbf{K},\mathbf{q})Q^{*}(\nu,\mu'',\mathbf{K}+\mathbf{q},\mathbf{q})\langle B^{+}_{\mu',\mathbf{K}+\mathbf{q}}B_{\mu'',\mathbf{K}+\mathbf{q}}\rangle$$
$$+\sum_{\mathbf{q},\mu',\mu''}\delta(E^{\mathbf{K}+\mathbf{q}}_{\mu''}-E^{\mathbf{K}}_{\mu}-\hbar\omega_{\mathbf{q}})Q(\mu,\mu'',\mathbf{K},\mathbf{q})Q^{*}(\nu,\mu',\mathbf{K}+\mathbf{q},\mathbf{q})\langle B^{+}_{\mu'',\mathbf{K}+\mathbf{q}}B_{\mu',\mathbf{K}+\mathbf{q}}\rangle\Bigg\}. \quad (28)$$

Here we have introduced the interband scattering rate defined as

$$\Gamma_{inter}\equiv\pi\sum_{\mathbf{q},\mu'}|Q(\mu,\mu',-\mathbf{q},\mathbf{q})|^{2}\delta(E^{0}_{\mu}-E^{-\mathbf{q}}_{\mu'}-\hbar\omega_{\mathbf{q}}) \quad (29)$$

and the intraband scattering rate defined as

$$\Gamma_{intra}(\mathbf{K})\equiv\pi\sum_{\mathbf{q},\mu'}\delta(E^{\mathbf{K}}_{\nu}-E^{\mathbf{K}-\mathbf{q}}_{\mu'}-\hbar\omega_{\mathbf{q}})|Q(\nu,\mu',\mathbf{K}-\mathbf{q},\mathbf{q})|^{2}$$
$$+\delta(E^{\mathbf{K}}_{\mu}-E^{\mathbf{K}-\mathbf{q}}_{\mu'}-\hbar\omega_{\mathbf{q}})|Q(\mu,\mu',\mathbf{K}-\mathbf{q},\mathbf{q})|^{2}. \quad (30)$$

C. Numerical implementation

Using Eqs. (5), (17), and (27), we can easily obtain the LO-phonon-induced interband polarization. However, even employing the Markov approximation, it is very computationally time consuming to keep track of the innumerable scattering processes in order to obtain the intraband polarization according to Eqs. (15), (18), and (28). There have been a number of calculations[25,27,28] that use Monte Carlo and related techniques within the Boltzmann or SBE formalisms to enable the inclusion of all of the relevant scattering events and density matrix elements. However, in essentially all experiments measuring THz emission due to BO's, the signal is only detectable over times on the order of a few picoseconds and so we are not interested in the long-time response. Thus, to simplify the intraband calculation, we limit the number of scattering events undergone by a given exciton. As we shall demonstrate, this approximation is valid over times long enough to determine an initial decoherence time.

We now turn to the approximations used in the calculation of the evolution of the intraband polarization. Since the $\mathbf{K}=\mathbf{0}$ excitons are initially optically excited, we need to consider the contributions from excitons with $\mathbf{K}=\mathbf{0}$. We also need to consider the contributions from $\mathbf{K}\neq\mathbf{0}$ excitons that have been scattered via phonons from $\mathbf{K}=\mathbf{0}$. So the total intraband polarization can be separated into two parts as

$$\mathbf{P}_{intra}=\frac{1}{V}\sum_{\mu,\nu}\mathbf{G}_{\mu\nu}\langle B^{+}_{\mu,0}B_{\nu,0}\rangle+\sum_{\mu,\nu}\mathbf{G}_{\mu\nu}S_{\mu,\nu}, \quad (31)$$

with

$$S_{\mu,\nu}\equiv\sum_{\mathbf{K}\neq 0}\langle B^{+}_{\mu,\mathbf{K}}B_{\nu,\mathbf{K}}\rangle. \quad (32)$$

The equations of motion for the two parts are

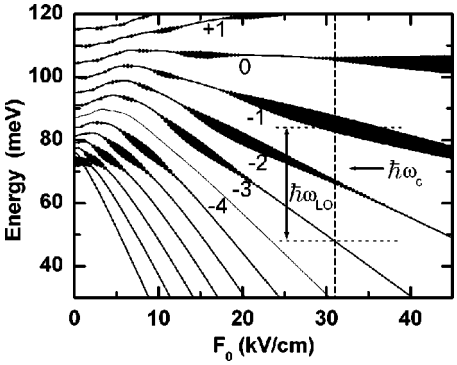

FIG. 1. The exciton energy levels (relative to the band gap of bulk GaAs) as a function of the dc electric field F_0 for the 50/15 superlattice discussed in the text. The number below each curve gives the quantum number ν for the excitonic state. The solid circles on each curve have diameters that are proportional to the optical oscillator strength of the given state. The vertical dashed line indicates the field at which the dynamical calculations are performed. Also indicated on the plot are the central frequency ω_c of the exciting laser pulse and the energy $\hbar\omega_{LO}$ of a LO phonon.

$$i\hbar\frac{d\langle B^+_{\mu,0}B_{\nu,0}\rangle}{dt}=[E^0_\nu-E^0_\mu-i\Gamma_{intra}(0)]\langle B^+_{\mu,0}B_{\nu,0}\rangle + \mathbf{E}_{opt}\cdot[M^*_\mu\langle B_{\nu,0}\rangle - M_\nu\langle B^+_{\mu,0}\rangle], \quad (33)$$

and for $\mathbf{K}\neq\mathbf{0}$

$$i\hbar\frac{d\langle B^+_{\mu,\mathbf{K}}B_{\nu,\mathbf{K}}\rangle}{dt}=[E^{\mathbf{K}}_\nu-E^{\mathbf{K}}_\mu-i\Gamma_{intra}(\mathbf{K})]\langle B^+_{\mu,\mathbf{K}}B_{\nu,\mathbf{K}}\rangle + i\pi\Bigg\{\sum_{\mu',\mu''}\delta(E^0_{\mu''}-E^{\mathbf{K}}_\nu-\hbar\omega_{-\mathbf{K}}) \times Q(\mu,\mu',\mathbf{K},-\mathbf{K})Q^*(\nu,\mu'',0,-\mathbf{K}) \times\langle B^+_{\mu',0}B_{\mu'',0}\rangle+\sum_{\mu',\mu''}\delta(E^0_{\mu''}-E^{\mathbf{K}}_\mu -\hbar\omega_{-\mathbf{K}})Q(\mu,\mu'',\mathbf{K},-\mathbf{K}) \times Q^*(\nu,\mu',0,-\mathbf{K})\langle B^+_{\mu'',0}B_{\mu',0}\rangle\Bigg\}. \quad (34)$$

The optically created excitons with $\mathbf{K}=\mathbf{0}$ are scattered to $\mathbf{K}\neq\mathbf{0}$ states with smaller internal number (down the WS ladder) via the emission of the phonons. Under the condition that phonon absorption is negligible the chance that the excitons are scattered back to their original states is energetically almost impossible. Thus in Eq. (33) it is seen that only the scattering-out contributions due to emission of optical phonons are taken into account. For the $\mathbf{K}\neq\mathbf{0}$ part, it should be noted that in the scattering-in contribution [the last two sums in Eq. (34)] we have only considered contributions from excitons with $\mathbf{K}=\mathbf{0}$; that is, we neglect the multiple-scattering processes, wherein excitons are scattered out of $\mathbf{K}=\mathbf{0}$ into $\mathbf{K}'\neq\mathbf{0}$ and subsequently into $\mathbf{K}''\neq\mathbf{0}$. This approximation is valid for times on the order of the decoherence time that we are interested in. We still need to determine $\Gamma_{intra}(\mathbf{K}\neq\mathbf{0})$. In order to simplify the calculations, we neglect the $\mathbf{K}$ dependence of Γ_{intra}. We have found that $\Gamma_{intra}(\mathbf{K}\neq\mathbf{0})$ is much smaller than $\Gamma_{intra}(0)$. Here we make the assumption that $\Gamma_{intra}(\mathbf{K}\neq\mathbf{0})=\Gamma_{intra}(0)$, which will thus give a T_{intra} that is always less than the true T_{intra}, i.e., *our calculation will return a lower bound on* T_{intra}. With this approximation, we can perform the sum over $\mathbf{K}$ in Eq. (32). This assumption greatly simplifies the calculations and, as we will show later, has little influence on the THz results. The resulting equation of motion for $S_{\mu,\nu}$ then reads

$$i\hbar\frac{dS_{\mu,\nu}}{dt}=[E^0_\nu-E^0_\mu-i\Gamma_{intra}(0)]S_{\mu,\nu}+i\pi\Bigg\{\sum_{\mu',\mu'',\mathbf{K}}\delta(E^0_{\mu''} -E^{\mathbf{K}}_\nu-\hbar\omega_{-\mathbf{K}})Q(\mu,\mu',\mathbf{K},-\mathbf{K})Q^*(\nu,\mu'',0,-\mathbf{K}) \times\langle B^+_{\mu',0}B_{\mu'',0}\rangle+\sum_{\mu',\mu'',\mathbf{K}}\delta(E^0_{\mu''}-E^{\mathbf{K}}_\mu-\hbar\omega_{-\mathbf{K}}) \times Q(\mu,\mu'',\mathbf{K},-\mathbf{K})Q^*(\nu,\mu',0,-\mathbf{K}) \times\langle B^+_{\mu'',0}B_{\mu',0}\rangle\Bigg\}. \quad (35)$$

Once we obtain the intraband polarization given by Eq. (31), we can calculate the THz signal by taking the second derivative of the intraband polarization.

III. NUMERICAL RESULTS AND DISCUSSION

We consider the heavy-hole excitons in a GaAs/$Ga_{0.7}Al_{0.3}As$ superlattice structure with a 50 Å well width and a 15 Å barrier width. The material parameters employed are the same as those given in Ref. 40. Using these parameters and calculations of the z-dependent excitonic dispersion,[41] we use $M_z=0.444$ and $M_\parallel=0.201$ for the c.m. effective masses. The resulting electron-hole miniband for this structure has a width of 75 meV, which is significantly larger than the LO phonon energy of 36 meV in GaAs. At low temperatures and in the low-density regime, exciton-acoustic-phonon interactions take place over times on the order of a few hundred picoseconds, so in a good quality superlattice, the LO phonon interaction will be the most important process for the loss of coherence. The calculations are performed using 21 basis states and we use GaAs parameters $\epsilon_\infty=10.92$, $\epsilon_s=12.9$, and $\hbar\omega_{LO}=36$ meV.

The $1s$ exciton energy levels as a function of the dc electric field are shown in Fig. 1, as calculated using the method of Dignam and Sipe.[40] The energy levels are labeled by the index ν which corresponds to the free particle WSL index n when the field is relatively high. More exactly, the expectation value of the electron-hole separation is given approximately by νd in the high-field limit. We denote the states by $|\nu\rangle$ for simplicity. We can see that the excitonic energy levels differ substantially from those of the single-particle Stark ladder levels, which would appear as a set of straight lines

with energy separations of $eF_o d$, all converging to a point at $F_0=0$. Because the effect of the electron-hole Coulomb interaction on the energy is different for the different states—i.e., the exciton binding energies for states with different ν are different—the separation, $E_{\nu+1}(F_0)-E_\nu(F_0)$, between adjacent energy levels is not $eF_0 d$, but is dependent on ν. We represent the oscillator strength of a given energy level at a given electric-field strength in Fig. 1 by a solid circle with a diameter that is proportional to the oscillator strength.

Now, we wish to consider a situation where the phonon-induced decoherence is large. Thus, in the following, we take the field to be $F_0=31$ kV/cm. As can be seen from Fig. 1, in this case, the separation between excitonic WSL states is approximately equal to $\hbar\omega_{LO}/2$. Thus, the dominant phonon-induced transitions will be $|\nu\rangle$ to $|\nu-2\rangle$. At this field strength, the $|-1\rangle$ and $|-2\rangle$ states have large oscillator strengths. Thus, to create an initial Bloch-oscillating state that is roughly an equal superposition of these two states, we center the optical pulse at an energy $\hbar\omega_c=E_{gap}^{GaAs}+71$ meV (see Fig. 1), and take the spectral full width at half maximum (FWHM) to be 15.5 meV (temporal FWHM of 118 fs). With this excitation energy, the $1s$ exciton population density created will be much larger than that of the unbound electron-hole pairs as discussed earlier.

Turning first to the calculation of the interband dynamics, we see from Eq. (27) that the interband polarization undergoes a simple exponential decay with a time constant given by $T_{inter}=1/\Gamma_{inter}$. Using the above parameters, we find that the interband decoherence time is $T_{inter}=2.5$ ps.

We now turn to the results for the intraband polarization. To aid in the discussion of the results, we present in Fig. 2 the calculated intraband polarization with differing levels of approximation. In Fig. 2(a), we present the intraband polarization neglecting the exciton-phonon interaction altogether. As can be seen, the polarization oscillates without decay at the Bloch frequency given by $\omega=\omega_{-1}-\omega_{-2}$. The dc contribution to the polarization is due to the dipole moment of the excitonic states, which is given roughly by $e\nu d$. Figure 2(b) shows the case where we add in the exciton-phonon interaction but only take into account the contributions of excitons with $\mathbf{K}=\mathbf{0}$. We find that both the dc and oscillating components of the intraband polarization decay rapidly to zero with a time constant of $1/\Gamma_{intra}(0)=T_{inter}/2$. Thus, we see that when the $\mathbf{K}\neq\mathbf{0}$ excitons are neglected, the system is in the so-called coherent limit. This is to be expected because in this case we only have a scattering-out term. Thus, the equations of motion for the intraband polarization to second order are identical to what one would obtain by simply employing the factorization $\langle B_{\mu,\mathbf{K}}^{+}B_{\nu,\mathbf{K}}\rangle=\langle B_{\mu,\mathbf{K}}^{+}\rangle\langle B_{\nu,\mathbf{K}}\rangle$. Therefore, the deviation from the coherent limit is directly related to the continuing coherence found in scattered excitons as we will now show.

In Figs. 2(c) and 2(d) we consider the contributions of excitons with $\mathbf{K}\neq\mathbf{0}$ to $\mathbf{P}_{intra}$. First, in Fig. 2(c), we exclude the decay term for the $\mathbf{K}\neq\mathbf{0}$ excitons by setting $\Gamma_{intra}(0)=0$ in Eq. (35). As expected, the intraband polarization changes dramatically. There are three main differences in the polarization in comparison to Fig. 2(b). First, rather than decaying, the dc component of the intraband polarization actually increases with time. This is due to the scattering of the excitons to states with larger $|\nu|$ and hence larger permanent intraband dipole. This reaches a roughly constant value eventually, because we have only allowed for single-scattering events. In a real system, of course, the long-time dependence of this dc component will depend on the boundaries of the superlattice. As we are only interested in the short-time response (less than a few picoseconds), we shall not discuss this issue further in this paper. The second feature of note is that there appears to be a beating phenomenon occurring. This is due to the fact that the excitons are scattered into the $|-3\rangle$ and $|-4\rangle$ states and the energy separation between these states is slightly different from that between the optically populated $|-1\rangle$ and $|-2\rangle$ states. Thus the $\mathbf{K}=\mathbf{0}$ and $\mathbf{K}\neq\mathbf{0}$ contributions to $\mathbf{P}_{intra}$ oscillate at slightly different frequencies, leading to beating. Finally, the intraband polarization in Fig. 2(c) decays much more slowly than in Fig. 2(b). This is the key result, and is due to the contributions of the $\mathbf{K}\neq\mathbf{0}$ excitons. In fact, at times larger than about 5 ps, the entire signal is essentially due to the $\mathbf{K}\neq\mathbf{0}$ excitons. This is

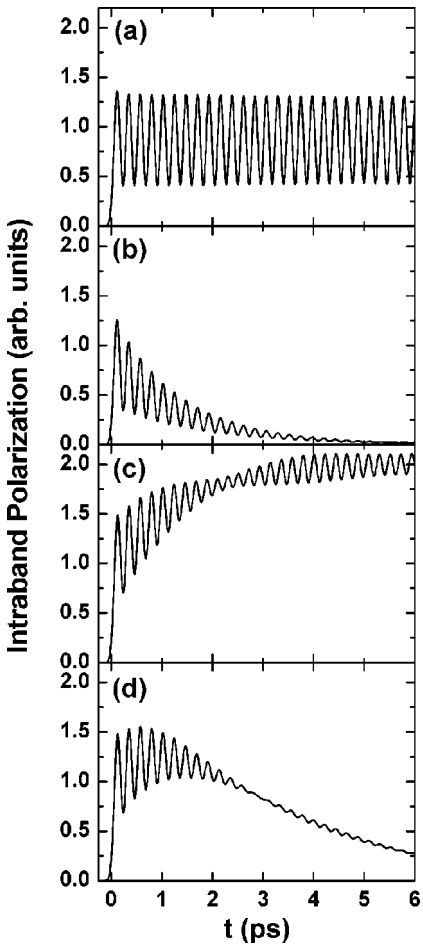

FIG. 2. Temporal evolution of the intraband polarization for four different cases: (a) without exciton-phonon interaction, (b) with contributions only from $\mathbf{K}=\mathbf{0}$ excitons, (c) with contributions from both $\mathbf{K}=\mathbf{0}$ and $\mathbf{K}\neq\mathbf{0}$ excitons, but no decay term of $\mathbf{K}\neq\mathbf{0}$, and (d) the full result using Eq. (35).

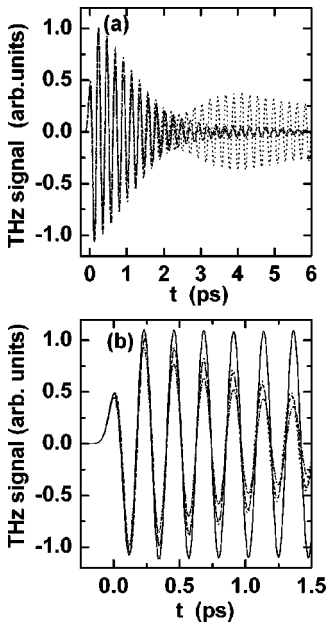

FIG. 3. Temporal evolution of the THz signal: (a) long-time and (b) short-time behavior. The solid line corresponds to the case without exciton-phonon interaction, the dash-dotted line corresponds to the case with contributions only from $\mathbf{K}=\mathbf{0}$ excitons, the dotted line corresponds to the case with contributions from both $\mathbf{K}=\mathbf{0}$ and $\mathbf{K}\neq\mathbf{0}$ excitons, but no decay term of $\mathbf{K}\neq\mathbf{0}$, and the dashed line corresponds to the full result using Eq. (35). For clarity, the solid line is omitted from (a).

not yet a fully realistic situation, because we have not included the decay of the $\mathbf{K}\neq\mathbf{0}$ excitonic contribution to the polarization. In Fig. 2(d) we add in the decay of the $\mathbf{K}\neq\mathbf{0}$ excitons and use the full dynamic equation, Eq. (35). As can be seen, this results in the decay of both the dc and oscillating components of the intraband polarization. At later times, the polarization decays at the same rate as in Fig. 2(b), because we have made the approximation that $\Gamma_{intra}(\mathbf{K}\neq\mathbf{0})=\Gamma_{intra}(0)$.

We now turn from the intraband polarization to the calculated THz signal, as this is the more experimentally accessible quantity. For clarity, in Fig. 3(a), we ignore the plot for the case without the exciton-phonon interaction, which oscillates without decay at the Bloch frequency given by $\omega=\omega_{-1}-\omega_{-2}$. We note that in the case where we have used the full dynamics equation, the THz signal decays to zero at long times. As discussed above, the time for this decay is in fact a lower bound for the decoherence time, as we have overestimated the decay time for the $\mathbf{K}\neq\mathbf{0}$ excitons, and we have not included the contributions of excitons that have undergone a second scattering event. For times longer than about 1.5 ps, the effects of the quantum beating discussed above become very evident, which makes it very difficult to determine a decay time for the signal over long times. Thus, we estimate the decoherence times by fitting the signal to a damped sinusoid over the first 1.5 ps, before beating is important. The THz signal over this time range is plotted in Fig. 3(b). In the case where we only take into account the contributions of excitons with $\mathbf{K}=\mathbf{0}$, the decoherence time is found to be 1.25 ps, which is half of the interband polarization decoherence time, as expected. When we consider the contributions of excitons with $\mathbf{K}\neq\mathbf{0}$ but exclude the decay of the $\mathbf{K}\neq\mathbf{0}$ excitons, the THz signal oscillation amplitudes are greatly increased and the decoherence time is 2.2 ps. Finally, with the full calculation, there is only a slightly more rapid decay in the THz signal, yielding a decoherence time of 2.1 ps. This time is much larger than the coherent limit value of 1.25 ps. We therefore see that the persistence of the intraband coherence after phonon scattering is the source of the strong deviation of the intraband and interband decoherence times from the coherent limit as experimentally observed.

From the results in Fig. 3(b), we see that over the short times of interest, the scattering of the $\mathbf{K}\neq\mathbf{0}$ excitons has almost no effect on the decoherence. As discussed earlier, the full calculation provides a lower bound for the decay time, as it overestimates the decay of the contribution from the $\mathbf{K}\neq\mathbf{0}$ excitons. On the other hand, the calculation that neglects the scattering of the $\mathbf{K}\neq\mathbf{0}$ excitons altogether provides an upper bound for the decay time. Since these times differ by only 0.1 ps, this justifies our neglect of multiple-scattering events.

IV. CONCLUSIONS

In this paper, using an excitonic basis, we have presented a detailed analysis of the decoherence of the intraband polarization and THz emission due to the interaction of excitons with LO phonons in an optically excited BSSL. We have shown that the difference between the decoherence times of interband and intraband polarizations lies in the fact that the former is determined by the dynamics of the excitons with $\mathbf{K}=\mathbf{0}$, while the latter is determined by the dynamics of excitons both with $\mathbf{K}=\mathbf{0}$ and $\mathbf{K}\neq\mathbf{0}$. We emphasize that the contributions of excitons with $\mathbf{K}\neq\mathbf{0}$ greatly prolong the coherence of the intraband dynamics. As a result, the THz emission decoherence time is almost equal to the interband decoherence time, in qualitative agreement with experimental results. We have described the origin of this effect using the example of exciton-LO-phonon scattering. However the same basic mechanism will also apply to other types of scattering such as exciton-acoustic-phonon scattering and exciton-exciton scattering, for example. It will not apply to pure dephasing due to inhomogeneities in the system, but will apply to some degree to any decoherence phenomenon where the center-of-mass wave vector is changed by a scattering event.

The experiments modeled in this work were for excitation conditions for which predominantly $1s$ excitons were optically excited. However, if one excites the superlattice with a laser pulse that has a central frequency centered above the energy of the $n=0$ $1s$ excitonic level, then continuum states will also contribute significantly to the intraband polarization.[33,34] In a recent publication,[34] we calculated the intraband polarization due to bound *and continuum* excitonic states in the absence of carrier-phonon scattering. As future work, we plan to extend these calculations to include the effects of optical phonons on the continuum intraband dy-

namics. As the general formalism required to include the continuum states remains largely unchanged from the formalism presented in this work, we expect that the intraband decoherence times for continuum excitation will also be longer than one would expect from a simple extrapolation of the interband decoherence times. However, the size of the difference will depend on the details and quantitative results require a full calculation.

ACKNOWLEDGMENTS

We acknowledge use of the HPCVL computing facility at Queen's University and thank Gang Liu for help in producing parallel code. We also thank Margaret Hawton for fruitful discussions. This work was supported in part by PREA and by the Natural Sciences and Engineering Research Council of Canada.

[1] A.V. Kuznetsov, Phys. Rev. B **44**, 13 381 (1991).
[2] J. Schilp, T. Kuhn, and G. Mahler, Phys. Rev. B **50**, 5435 (1994).
[3] T. Meier, G. von Plessen, P. Thomas, and S.W. Koch, Phys. Rev. Lett. **73**, 902 (1994).
[4] Stefan Haas, Fausto Rossi, and Tilmann Kuhn, Phys. Rev. B **53**, 12 855 (1995).
[5] K. Leo, Semicond. Sci. Technol. **13**, 249 (1998).
[6] F. Wolter, R. Martini, S. Tolk, P. Harving Bolivar, H. Kurz, R. Hey, and H.T. Grahn, Superlattices Microstruct. **26**, 93 (1999).
[7] K. Hannewald, S. Glutsch, and F. Bechstedt, Phys. Rev. B **61**, 10 792 (2000).
[8] P.G. Huggard, C.J. Shaw, S.R. Andrews, J.A. Cluff, and R. Grey, Phys. Rev. Lett. **84**, 1023 (2000).
[9] T. Dekorsy, A. Bartels, H. Kurz, K. Köhler, R. Hey, and K. Ploog, Phys. Rev. Lett. **85**, 1080 (2000).
[10] B. Krummheuer, V.M. Axt, and T. Kuhn, Phys. Rev. B **65**, 195313 (2002).
[11] F. Rossi and T. Kuhn, Rev. Mod. Phys. **74**, 895 (2002).
[12] A. Vagov, V.M. Axt, and T. Kuhn, Phys. Rev. B **66**, 165312 (2002).
[13] M. Herbst, M. Glanemann, V.M. Axt, and T. Kuhn, Phys. Rev. B **67**, 195305 (2003).
[14] F. Bloch, Z. Phys. **52**, 555 (1928).
[15] G.H. Wannier, Phys. Rev. **117**, 432 (1960).
[16] E.E. Mendez, F. Agullo-Rueda, and J.M. Hong, Phys. Rev. Lett. **60**, 2426 (1988).
[17] P. Voisin, J. Bleuse, C. Bouche, S. Gaillard, C. Alibert, and A. Regreny, Phys. Rev. Lett. **61**, 1639 (1988).
[18] J. Feldmann, K. Leo, J. Shah, D.A.B. Miller, J.E. Cunningham, T. Meier, G. von Plessen, A. Schulze, P. Thomas, and S. Schmitt-Rink, Phys. Rev. B **46**, 7252 (1992).
[19] P. Leisching, P. Haring Bolivar, W. Beck, Y. Dhaibi, F. Brüggemann, R. Schwedler, H. Kurz, K. Leo, and K. Köhler, Phys. Rev. B **50**, 14 389 (1994).
[20] K. Leo, P. Haring Bolivar, F. Brüggemann, and R. Schwedler, Solid State Commun. **84**, 943 (1992).
[21] T. Dekorsy, P. Leisching, K. Köhler, and H. Kurz, Phys. Rev. B **50**, 8106 (1994).
[22] C. Waschke, H.G. Roskos, R. Schwedler, K. Leo, H. Kurz, and K. Köhler, Phys. Rev. Lett. **70**, 3319 (1993).
[23] H. Roskos, C. Waschke, R. Schwedler, P. Leisching, Y. Dhaibi, H. Hurz, and K. Köhler, Superlattices Microstruct. **15**, 281 (1994).
[24] T. Meier, G. von Plessen, P. Thomas, and S.W. Koch, Phys. Rev. Lett. **73**, 902 (1994); **51**, 14 490 (1995).
[25] T. Meier, F. Rossi, P. Thomas, and S.W. Koch, Phys. Rev. Lett. **75**, 2558 (1995).
[26] V.M. Axt, G. Bartels, and A. Stahl, Phys. Rev. Lett. **76**, 2543 (1996).
[27] F. Rossi, T. Meier, P. Thomas, S.W. Koch, P.E. Selbmann, and E. Molinari, Phys. Rev. B **51**, 16 943 (1995).
[28] Jörg Hader, Torsten Meier, Stephan W. Koch, Fausto Rossi, and Norbert Linder, Phys. Rev. B **55**, 13 799 (1997).
[29] J.M. Lachaine, Margaret Hawton, J.E. Sipe, and M.M. Dignam, Phys. Rev. B **62**, R4829 (2000).
[30] M.M. Dignam and M. Hawton, Phys. Rev. B **67**, 035329 (2003).
[31] Aizhen Zhang, Lijun Yang, and M.M. Dignam, Phys. Rev. B **67**, 205318 (2003).
[32] Margaret Hawton and M. M. Dignam, Phys. Rev. Lett. **91**, 267402 (2003).
[33] M. Dignam, J.E. Sipe, and J. Shah, Phys. Rev. B **49**, 10 502 (1994).
[34] Lijun Yang, Ben Rosam, Jean-Marc Lachaine, Karl Leo, and M. M. Dignam (unpublished).
[35] P.H. Bolivar, F. Wolter, A. Müller, H.G. Roskos, H. Kurz, and K. Köhler, Phys. Rev. Lett. **78**, 2232 (1997).
[36] R. Zimmermann, E. Runge, and V. Savona, *Quantum Coherence, Correlation and Decoherence in Semiconductor Nanostructures*, edited by Toshihide Takagahara (Elsevier Science, Oxford, 2003).
[37] Wei Min Zhang, Torsten Meier, Vladimir Chernyak, and Shaul Mukamel, Phys. Rev. B **60**, 2599 (1999).
[38] Margaret Hawton and Delene Nelson, Phys. Rev. B **57**, 4000 (1998).
[39] E. Molinari, in *Confined Electrons and Photons: New Physics and Applications*, edited by E. Burstein and C. Weisbuch (Plenum, New York, 1994).
[40] M.M. Dignam and J.E. Sipe, Phys. Rev. Lett. **64**, 1797 (1990); Phys. Rev. B **43**, 4097 (1991).
[41] M.M. Dignam and J.E. Sipe, Phys. Rev. B **41**, 2865 (1990).